EUROPEAN ORGANIZATION FOR NUCLEAR RESEARCH

CERN-EP/86-30
March 3rd, 1986

# RESULTS OF A 100 MHZ FADC SYSTEM BUILT IN FASTBUS USED BY THE UA2 VERTEX DETECTOR

F. Bourgeois[1], G. Carboni[4], T. Del Prete[4], G. De Palma[4], L. Fayard[3], D. Froidevaux[3], E. Iacopini[5], K. Jakobs[2], H. Plothow-Besch[2], G. Sauvage[3], M. Wunsch[2].

(Contribution to the Wire Chamber Conference, Vienna 1986)

ABSTRACT

The drift chambers of the UA2 vertex detector were equipped with a FASTBUS-based, 100 MHz FADC system for the 1985 run of the CERN $\bar{p}p$ collider. This was the first large-scale use of such a system. Pulse shaping and online zero suppression were used to reduce the total amount of data produced by the system. A substantial improvement with respect to the previously used system in the two-track separation was obtained with no loss in precision for the reconstructed coordinates. The drift time information was used to reconstruct transverse coordinates with a precision of ~ 145 μm (rms). The longitudinal coordinates were derived from charge division with a precision of better than 1% of the wire length. The two-track separation was 2.5 mm with an efficiency of 90%.

---

1. CERN, 1211 Geneva 23, Switzerland.
2. Institut für Hochenergiephysik der Universität Heidelberg, Schröderstrasse 90, 6900 Heidelberg, FRG.
3. LAL, Université de Paris-Sud, Orsay, France.
4. Universitá di Pisa and INFN, Via Livornese, S. Piero a Grado, Pisa, Italy.
5. Scuola Normale di Pisa and INFN, Via Livornese, S. Piero a Grado, Pisa, Italy.

## 1. INTRODUCTION

The UA2 detector [1] was designed to investigate $\bar{p}p$ interactions at the CERN SPS collider. Its main aims and its great successes are the detection of the weak gauge bosons and the study of the properties of hadron production [2,3]. In order to improve the tracking capability of the UA2 central detector, the two drift chambers (a total of 288 wires) were equipped with a 100 MHz Flash ADC (FADC) system for the 1985 $\bar{p}p$ collider run (see Fig. 1).

In the present paper, we describe the detector electronics in section 2, the channel by channel calibration in section 3, and the performances obtained with offline analysis in section 4.

## 2. THE DETECTOR ELECTRONICS

The UA2 central detector [4] consists of a set of 4 cylindrical proportional chambers with cathode strip readout (which provide a resolution along the wire of 1 mm) and 2 JADE type drift chambers with charge division readout. Each of the 2 drift chambers consists of 24 cells of 6 sense wires each (the wire length of the chambers are 1.5 m and 1.8 m, respectively). The particle trajectory is reconstructed in the transverse plane from the measurement of the drift time (typical drift times are less than 1 μs) and along the chamber axis from the charge division on the resistive sense wires (2070 Ω/m).

To have a good tracking capability it is necessary to measure both the pulse amplitude and its absolute time of arrival with good precision. Since interesting $\bar{p}p$ events have an average particle multiplicity of ~ 50, it is also necessary to discriminate multiple hits occurring on the same wire.

We have used the 100 MHz FADC system described in ref. 5, based on the TRW TDC1029 circuit. To match the pulse characteristics with the FADC design, we have also built two-pole shaping amplifiers/active drivers (AD) to drive the 85m 100Ω twisted pair cables between the ADs and the FADCs. The ADs differentiate the pulse from the chamber preamplifier [6] in such a way that the pulse at the FADC input port has a rise time of ~ 40 ns and a base-width ≤ 120 ns. Figure 2a shows a linearized multi-hit signal pulse (see section 4).

To expand the insufficient 6-bit TRW1029 dynamic range, the FADC was operated with the hyperbolic drive described in ref. 7. In this way, for a normalized input $x$ ($0 \leq x \leq 1$), the FADC output $y$ is

$$y = 63x / [1 - \alpha + \alpha x] \qquad (1)$$

where $\alpha$ is an adjustable constant. To get the same non-linear behaviour for all the FADCs, it has been necessary to compensate for the variation of the resistances of the FADC dividers (the resistances range from 40Ω to 50Ω) with suitable parallel resistors. They have been equalized to 40Ω ± 0.3Ω at the working temperature of 65°C ($\delta R/\delta T = 0.16$ Ω/°C). We have chosen for $\alpha$ the value $0.75 \pm 0.01$ which, according to eq. (1), expands the dynamic range by a factor 4. This dynamic range expansion results in an increase of the rounding error and implies a 5% error on the determination of the charge from a typical pulse.

Each wire is seen by two FADCs (Left and Right channel). Each 10 ns, the L and R pulse heights are written into a memory partitioned into 16 blocklets of 16 words each (1 word = 16 bits). The description of the encoding/decoding of the FADC information is given in ref. 5. Only the pulses for which the analog sum of the left and right channels exceeds a 6-bit programmable threshold value are considered. The information corresponding to each pulse is stored into a 16-word blocklet containing 12 successive samples of the pulse and 4 samples taken just before it exceeds the preset threshold (to monitor possible base-line shifts).

To fully exploit the FADC dynamic range, 6-bit programmable dc offsets can be added independently to the L and R signals. This operation does not affect the threshold rejection efficiency.

The FADC system was implemented in the FASTBUS standard. Thirty-two channels are grouped in a 2-unit wide FASTBUS module, the GATHER (see ref. 5). The 288 wires are digitized in 18 modules which are housed in two high power FASTBUS crates (1.5 KW).

The standard data acquisition of UA2 was implemented in a CAMAC-REMUS environment. A special REMUS interface, the Gather Fastbus Remus Processor (GFRP) [8], was designed and built to perform the FASTBUS readout and to load

the values of the threshold and offsets for each wire. The GFRP resides in the FASTBUS crate and upon the occurrence of a trigger, performs most of the decoding described in ref. 5 in a few microseconds. The number of words transferred to the REMUS port is therefore minimized. The total amount of data produced by the system for each event was typically ~ 20 kbytes.

## 3. THE ONLINE CALIBRATION

Each channel (of a total of 576) was calibrated individually. The threshold is determined by adjusting the rate of random hits (noise rate) to an acceptable level. As an example, Fig. 3a shows the measured noise rate as a function of the threshold setting for one wire. During data taking the noise rate was set to ~ 2%. The bias voltage was determined by measuring the residual pedestal (no signal at the FADC input) as a function of the baseline setting. This functional behavior was then fitted by a linear curve excluding the first few (non linear) bins. A typical baseline setting was 4 FADC counts. The electronics noise resulting in pedestal fluctuations was measured to be on the average 0.8 FADC counts. Figure 3b shows the measured residual pedestal as a function of bias setting together with the fitted linear curve. The typical bias setting is also indicated.

The hyperbolic response of each FADC channel can be described by a relation derived from eq. (1),

$$Q_{lin} = G \cdot 63N \,/\, (63 - \alpha N) - Ped \qquad (2)$$

where $Q_{lin}$ stands for the charge per time bin collected at either end of a wire, N for the number of non-linear FADC counts, and Ped for the linearized pedestal value. The slope parameter $\alpha$ and the gain parameter G of each individual channel are determined by injecting charges of different pulse heights at the input of the chamber preamplifier and measuring the corresponding FADC response. They are then fitted using relation (2). Figures 4a and 4b show the distribution of $\alpha$ and G, for the 144 channels on one side of the chamber.

Typical channel to channel variations (rms) of ~ 4% for the slope parameter and of ~ 17% for the gain measurement was observed. The average value of $\alpha$ was measured to be $0.773 \pm 0.001$ which is close to the expected value for an ideal FADC response. The pedestal and threshold settings, as well as the slope and gain parameters, were monitored regularly during data taking and were found to be remarkably stable.

## 4. THE OFFLINE ANALYSIS RESULTS

In the following, we describe the three parts of the offline analysis chain: the hit finding, the coordinate reconstruction in the transverse plane ($\phi$ coordinate) and the longitudinal coordinate reconstruction (z coordinate). For the offline analysis, linearized FADC signals were used. The linearized signals were computed by applying relation (2) to each time bin. To determine the quality of the results obtained (i.e. the accuracy in $\phi$ and in z, as well as the two-track separation), we compare the reconstructed drift chamber coordinates with tracks that were reconstructed by using only the 4 additional proportional chambers of the UA2 vertex detector.

The hit finding was done by using a differentiation method [9]. The differentiated signal is computed by taking the differences of the FADC contents in consecutive bins. As shown in Fig. 2b, hits are then defined as maxima in this differentiated spectrum above a certain threshold which was typically set to 5 counts. By using this method we were able to recognize multi-hits with a high efficiency. The efficiency as a function of hit separation is shown in Fig. 5. Two tracks separated by 2.5 mm are resolved with an efficiency of 90%.

The further analysis of the differentiated signal provides the determination of the drift time. The center of gravity of the maximum of the differentiated signal gives the best estimate of the drift time. The best results were obtained by using $\pm$ 2 bins around the maximum, where only consecutive bins above zero amplitude were taken into account. This method was applied to the FADC signal at the left and right ends of the wire. The mean value of the two times was used to reconstruct the $\phi$ coordinate. After applying corrections to take into account wire misalignments, drift velocity variations and differences in

cable length to each individual channel, we obtained a precision of ~ 145 μm (rms) for reconstructed coordinates.

For the reconstruction of the z coordinate, two cases have to be distinguished. The simplest case is a single hit produced by a track which is isolated in $\phi$. If two or more tracks are nearby in $\phi$, the FADC pulses overlap and must be unfolded to obtain the correct z coordinates. Furthermore, because of the small dynamic range of the 6 bit FADC, a non-negligible fraction of hits (13.2% for minimum bias events) have at least one FADC bin in overflow.

For single hits the charge is calculated as a sum over the bins around the maximum bin. Studies have shown that the optimum accuracy is reached if six bins are used as the integration range, three before and two after the maximum. Figure 6 shows the dependence of the z precision as a function of the total charge $Q_{tot}$. The observed flat behaviour at high values of $Q_{tot}$ can be explained by the non-linear FADC response. Furthermore, the precision was found to be relatively independent of the z coordinate. On average, the resolution was better than 1% of the wire length. Despite the fact that the accuracy of the FADCs was limited to 6 bits, the precision for reconstructed coordinates was similar to the 12 bit integrating system that was previously used. A substantial improvement (by a factor 3) of the two-track separation was obtained.

In order to deconvolute overlapping pulses, we have studied the pulse shape of the FADC signals. A typical pulse has a rise time of ~ 40 ns and a length of ~ 120 ns. Detailed studies of the pulse shape have been performed for different intervals of $\phi$, z, and the total charge. We find that the pulse shape is well described by a single reference shape in all cases. This reference shape was therefore used to deconvolute overlapping pulses. Fig. 7 shows the accuracy in z as a function of the time separation between two hits. It is shown for the first and the second hits, separately. The resolution in z varies by about a factor of 6 when the intervall between the overlapping pulses varies from 120 ns (~ 6 mm) to 50 ns (2.5 mm). The accuracy for the first hit is significantly better than for the second hit because the leading edge of the first pulse is not influenced by the following one.

Saturated pulses were recovered by using the reference pulse method. For the comparison with the reference pulse, only the non saturated bins were taken

into account. It was possible to recover charges with up to nine saturated time bins. The variation of the z accuracy as a function of the number of saturated bins is shown in Fig. 8. The z accuracy varies from 1.2% to 7% when the number of saturated bins varies from one to nine.

## 5. CONCLUSIONS

For the first time, a FASTBUS implementation of a 100 MHz FADC system was used in a large-scale experiment. Pulse shaping and online zero suppression was used to substantially reduce the total quantity of data. The 576 channels were calibrated individually.

Resolutions of ~ 145 μm (rms) in the transverse coordinate and less than 1% of the wire length in the longitudinal coordinate were achieved. A two-track separation of 2.5 mm with an efficiency of 90% was obtained.

ACKNOWLEDGEMENTS

We deeply thank the UA2 Collaboration for the strong support they have given us to obtain a working FADC system. In particular, we would like to thank the UA2 members J. R. Hansen and L. Mapelli for their contribution to the online data acquisition and G. Parrour and J. P. Repellin for their contribution to the offline analysis. We also would like to thank L. Bonnefoy for his help in mounting and testing the Active Driver units. We would like to thank the OME EF group and the EP Pool for their assistance.

REFERENCES


[1] B. Mansoulié, The UA2 apparatus at the CERN $\bar{p}p$ Collider, Proc. 3rd Moriond workshop on $\bar{p}p$ physics (Editions Frontière, Dreux, 1983) p. 609.

[2] M. Banner et al., UA2 Collaboration, Phys. Lett. 122B (1983) 476;
P. Bagnaia et al., UA2 Collaboration, Phys. Lett. 129B (1983) 130
P. Bagnaia et al., UA2 Collaboration,
Z. Phys. C, Particles and Fields 24 (1984) 1
J. A. Appel et al., UA2 Collaboration, CERN EP/85-166.

[3] M. Banner et al., UA2 Collaboration, Phys. Lett. 118B (1982) 203;
P. Bagnaia et al., UA2 Collaboration, Phys. Lett. 144B (1984) 283
P. Bagnaia et al., UA2 Collaboration, Phys. Lett. 144B (1984) 291
J. A. Appel et al., UA2 Collaboration, Phys. Lett. 160B (1985) 349.

[4] M. Dialinas et al., The vertex detector of the UA2 experiment, LAL-RT/83-14 (Orsay, 1983).

[5] F. Bourgeois, Proposal for a Fast, Zero Supressing circuit for Digitization of Analog Pulses Over Long Memory Times, Nucl. Instrum. Methods 219 (1984) 153;
F. Bourgeois et al., IEEE Trans. Nucl. Sci. NS-32 (1985) 631.

[6] A. Hrisoho and K. Truong, LAL-RT/79-4 (Orsay, 1979).

[7] B.Hallgren and H.Verweij, New Developments in time and pulse height digitizers, IEEE Trans. Nucl. Sci. NS-27 (1980) 1.

[8] G. De Palma, Thesis, Pisa University, 1985.

[9] D. Schaile, O. Schaile and J. Schwarz, CERN-EP/85-95.

FIGURE CAPTIONS

Fig. 1 Artists view of the two drift chambers of the UA2 vertex detector and of their readout.

Fig. 2a Linearized FADC pulse showing a multi-hit pattern

Fig. 2b Differentiated FADC signal

Fig. 3a Noise rate as a function of threshold setting for one wire

Fig. 3b Residual pedestal as a function of bias setting for one wire

Fig. 4a Distribution of the slope parameter $\alpha$ for 144 channels

Fig. 4b Distribution of the gain parameter G for 144 channels

Fig. 5 Efficiency as a function of the two track separation

Fig. 6 Z accuracy for single hits as a function of the total charge

Fig. 7 Z accuracy for two overlapping pulses as a function of the time separation

Fig. 8 Z accuracy from saturated pulses as a function of the number of saturated FADC time bins

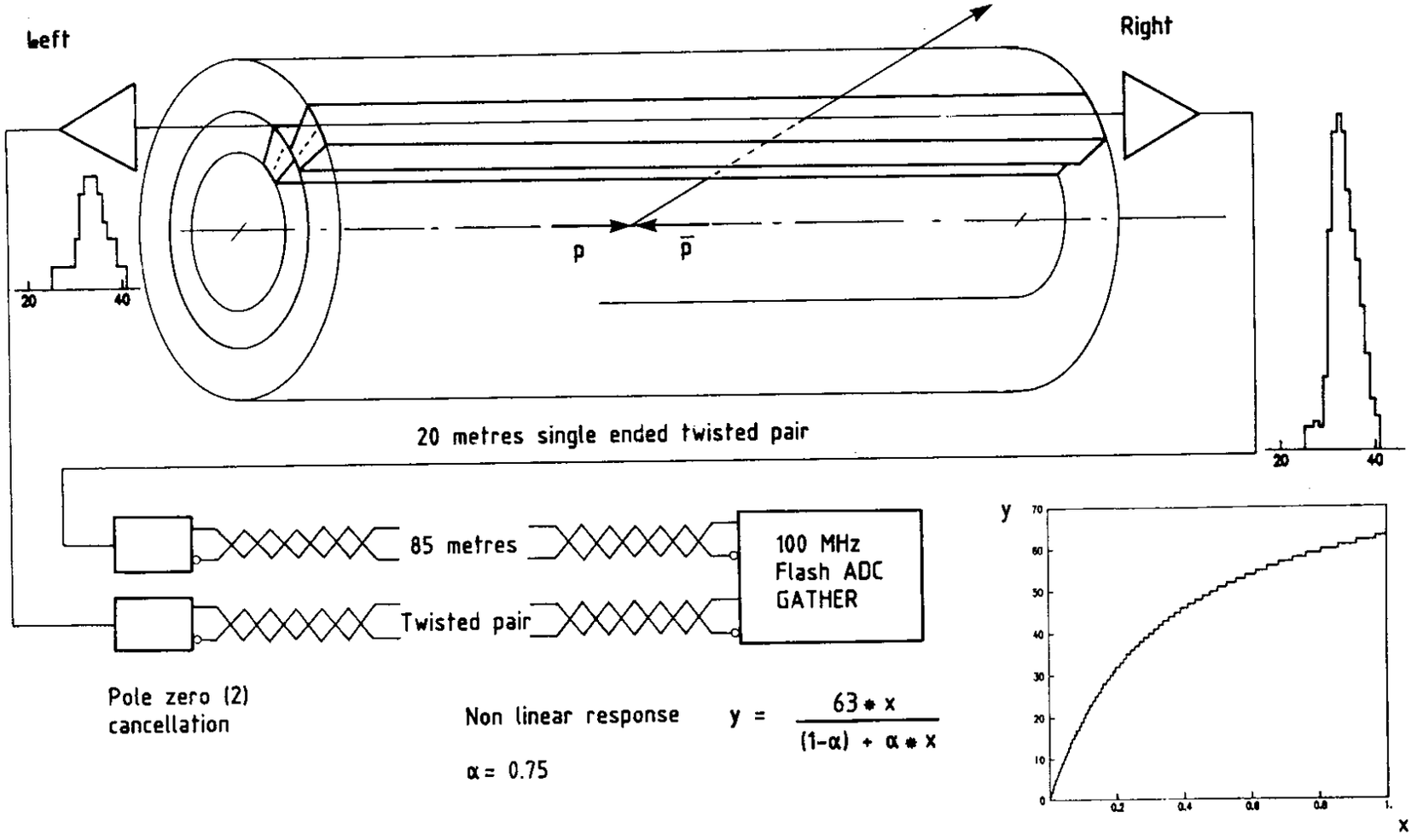
Left
Right
p
$\bar{p}$
20
40
20 metres single ended twisted pair
85 metres
Twisted pair
100 MHz
Flash ADC
GATHER
Pole zero (2)
cancellation
Non linear response
$y = \frac{63 * x}{(1-\alpha) + \alpha * x}$
$\alpha = 0.75$
y
x

Fig. 1

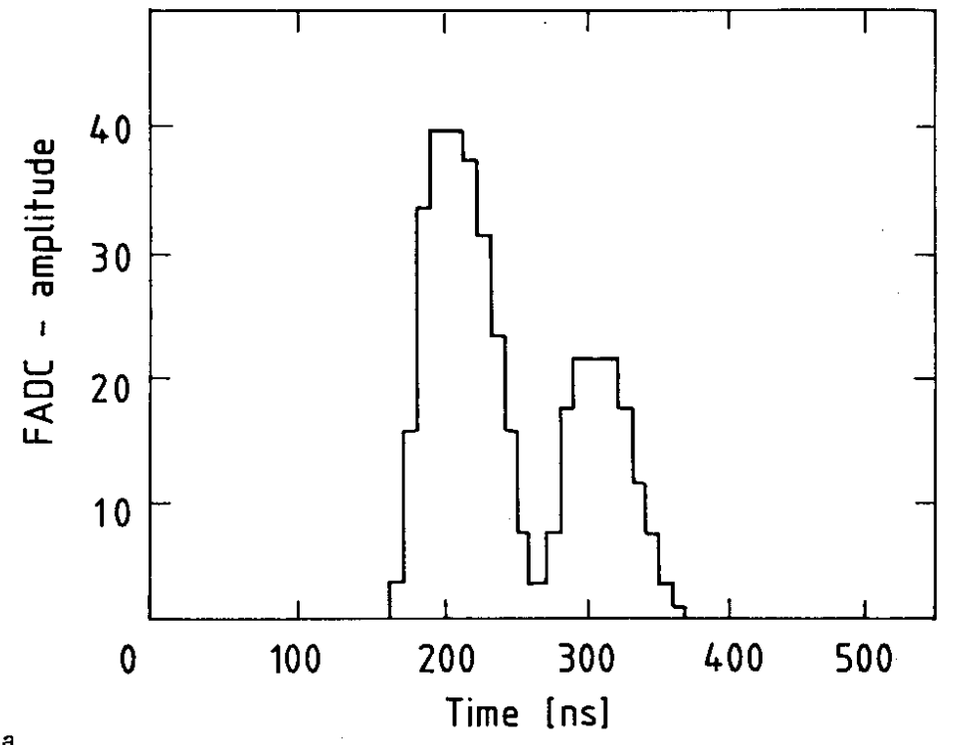
FADC - amplitude
40
30
20
10
0
100
200
300
400
500
Time [ns]

Fig. 2a

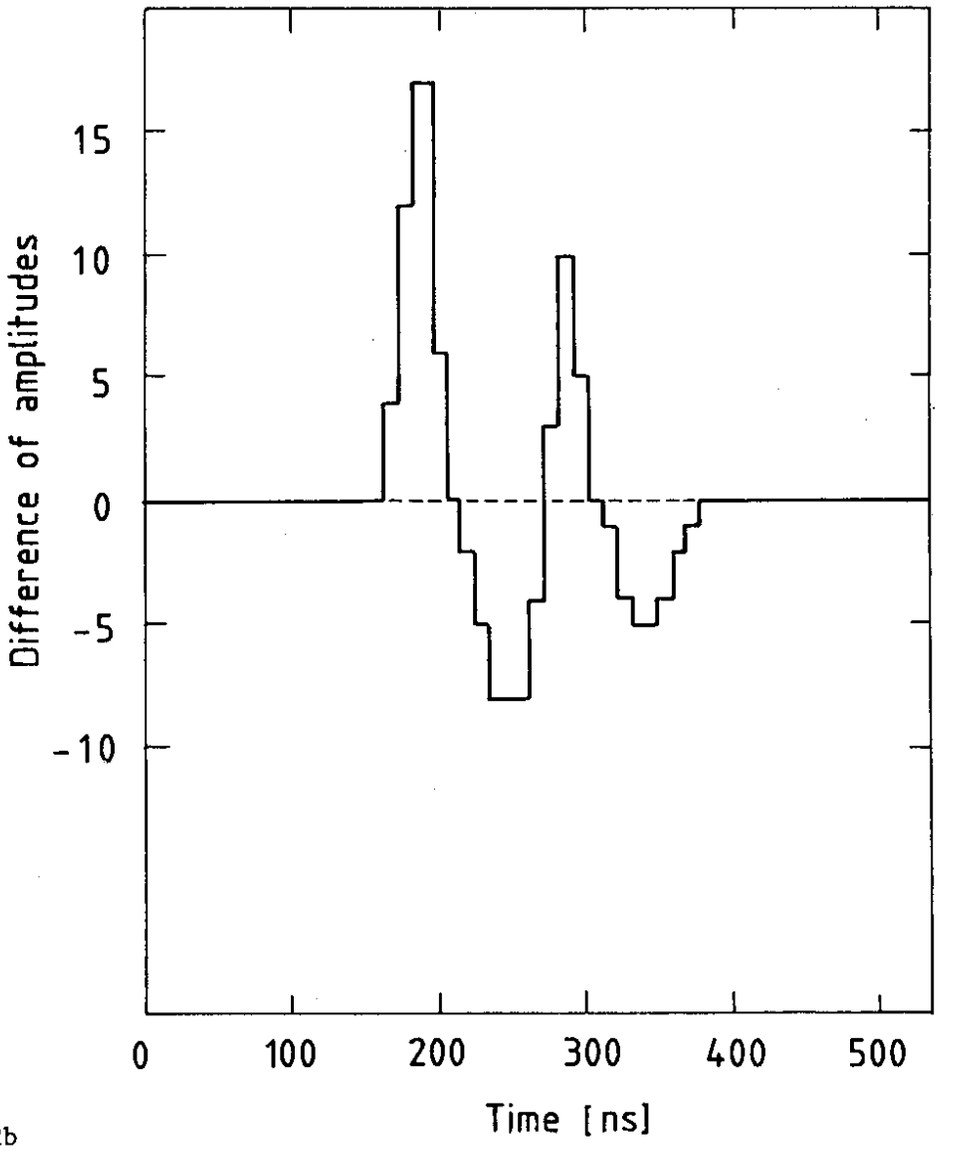
Difference of amplitudes
15
10
5
0
-5
-10
0
100
200
300
400
500
Time [ns]

Fig. 2b

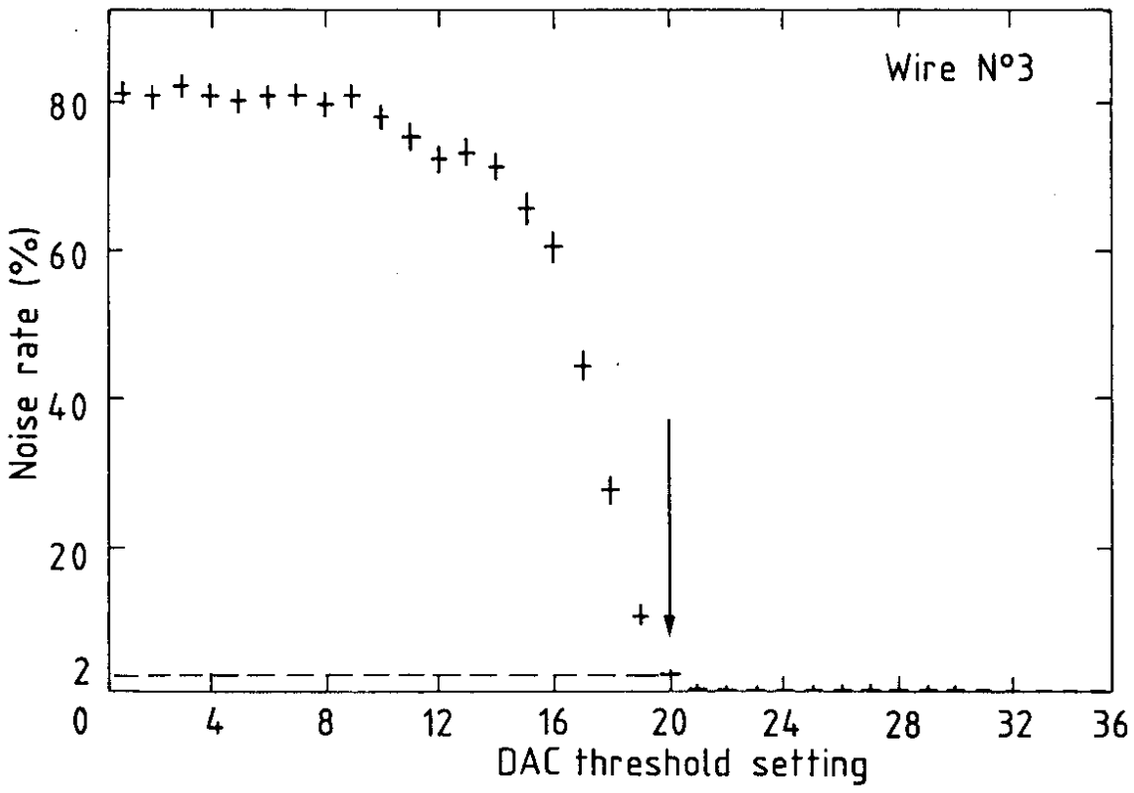
Wire N°3
Noise rate (%)
80
60
40
20
2
0
4
8
12
16
20
24
28
32
36
DAC threshold setting

Fig. 3a

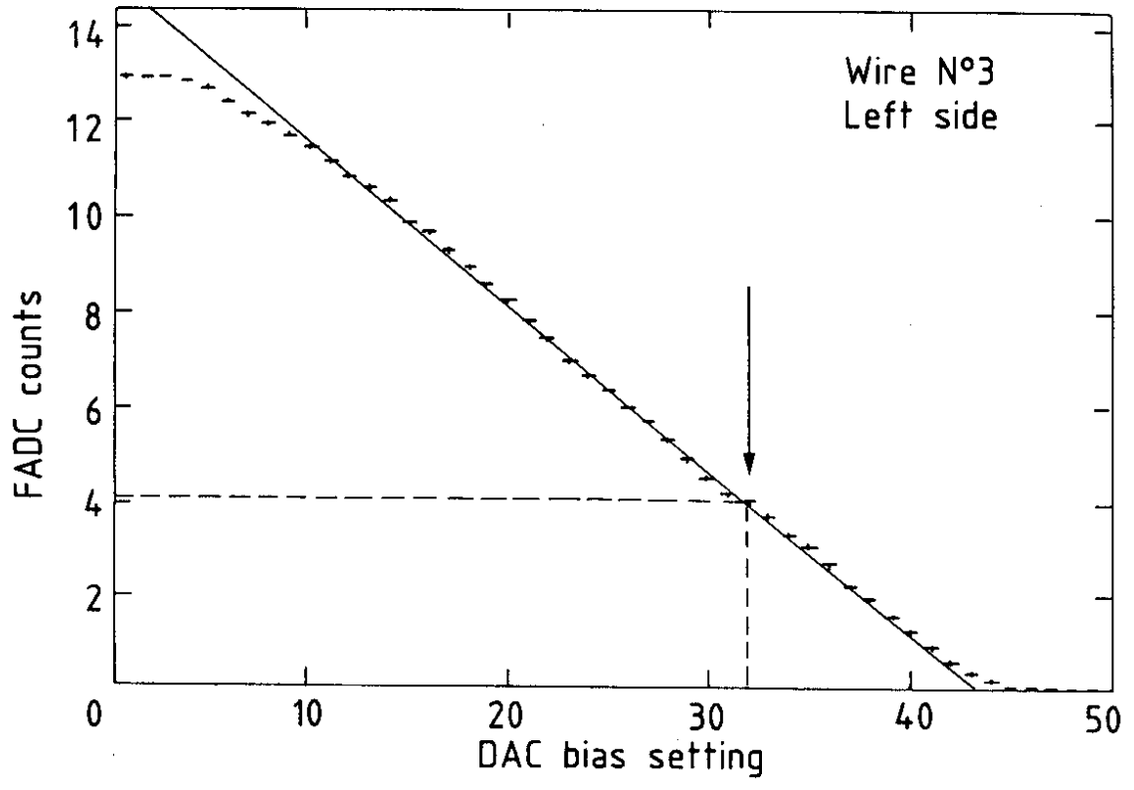
Wire N°3
Left side
FADC counts
14
12
10
8
6
4
2
0
10
20
30
40
50
DAC bias setting

Fig. 3b

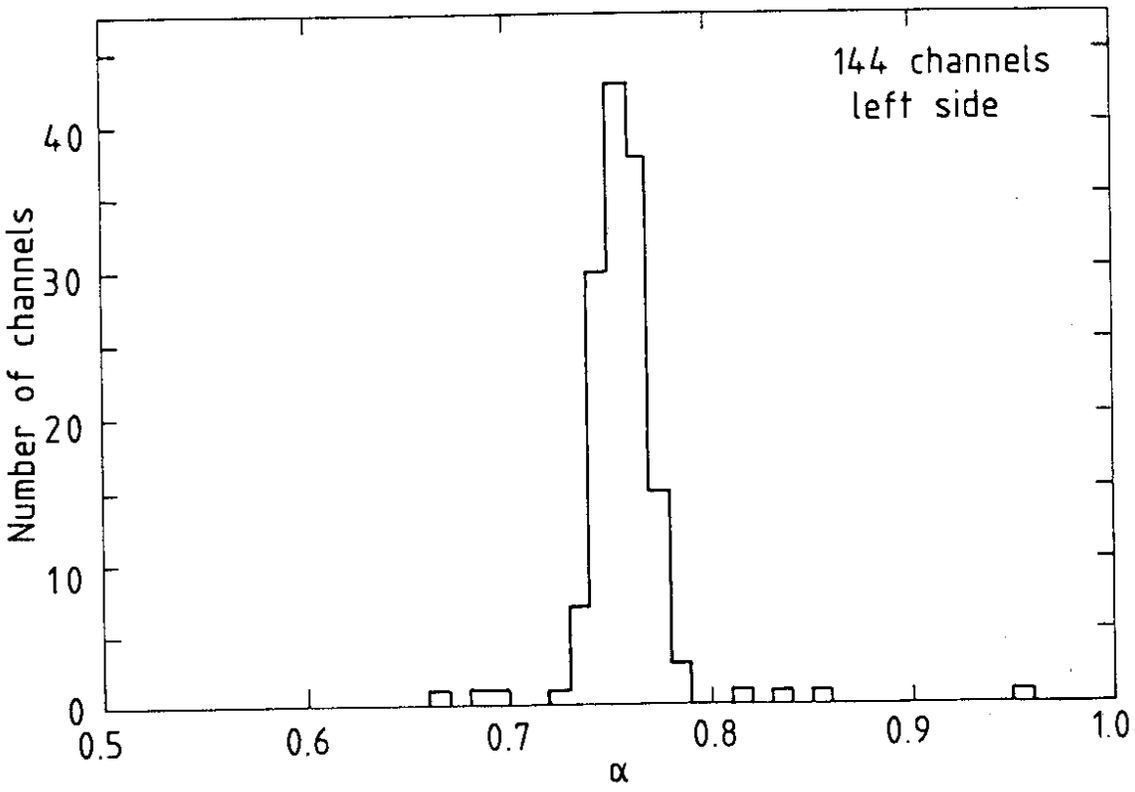
144 channels
left side
Number of channels
0
10
20
30
40
0.5
0.6
0.7
0.8
0.9
1.0
α

Fig. 4a

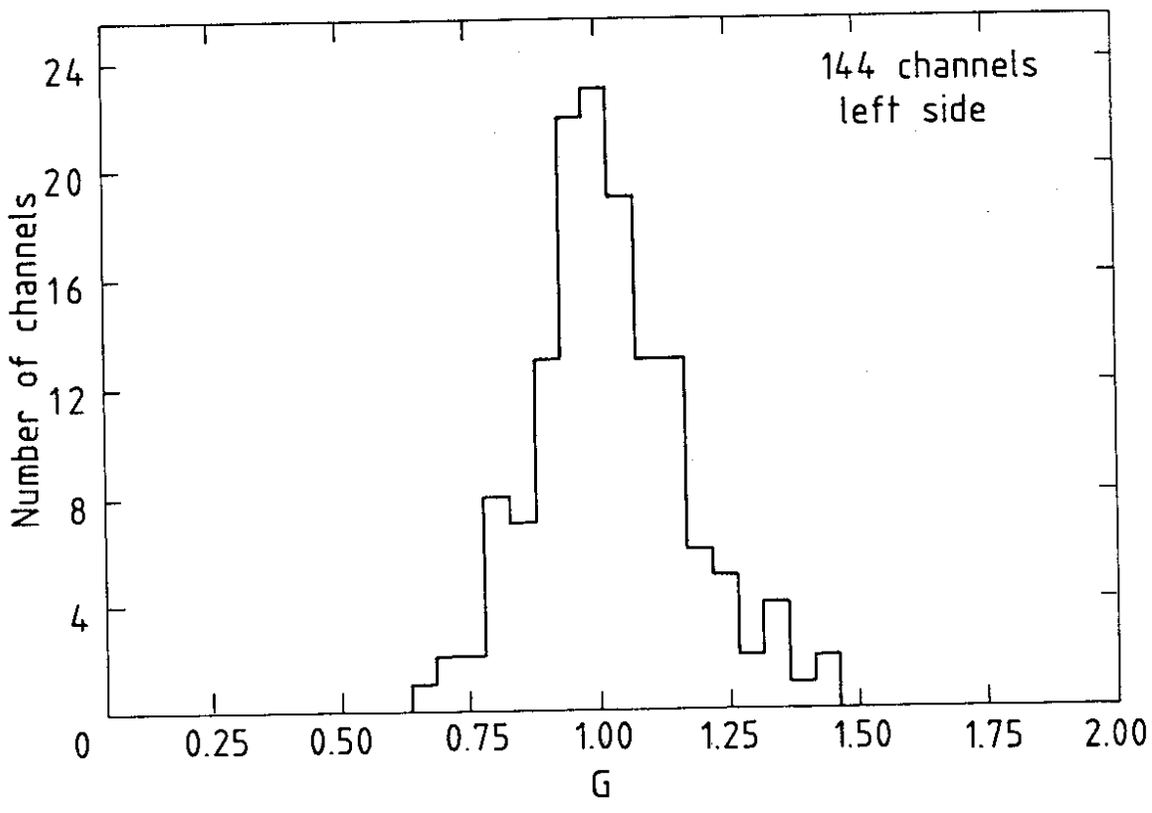
144 channels
left side
Number of channels
0
4
8
12
16
20
24
0
0.25
0.50
0.75
1.00
1.25
1.50
1.75
2.00
G

Fig. 4b

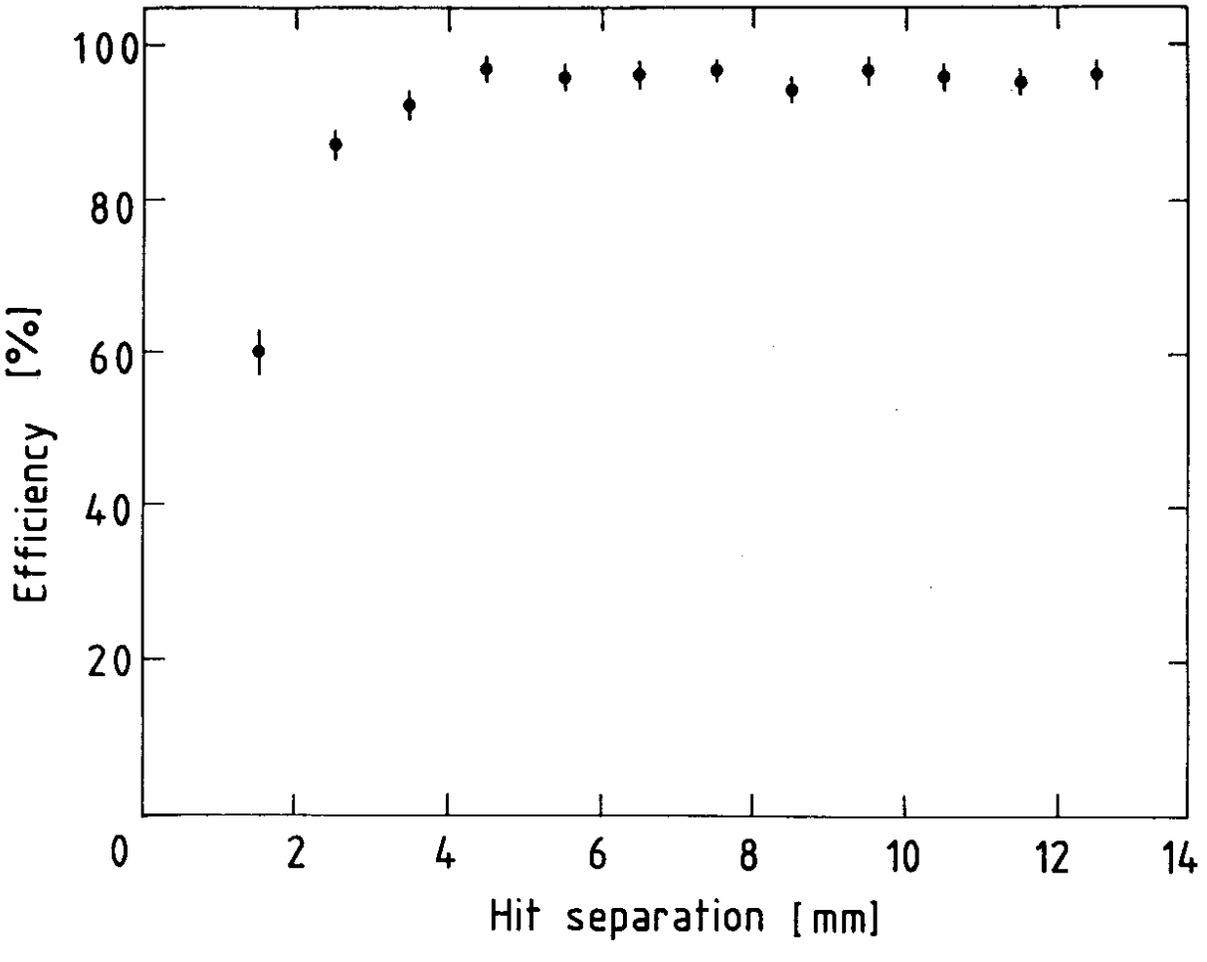


Fig. 5

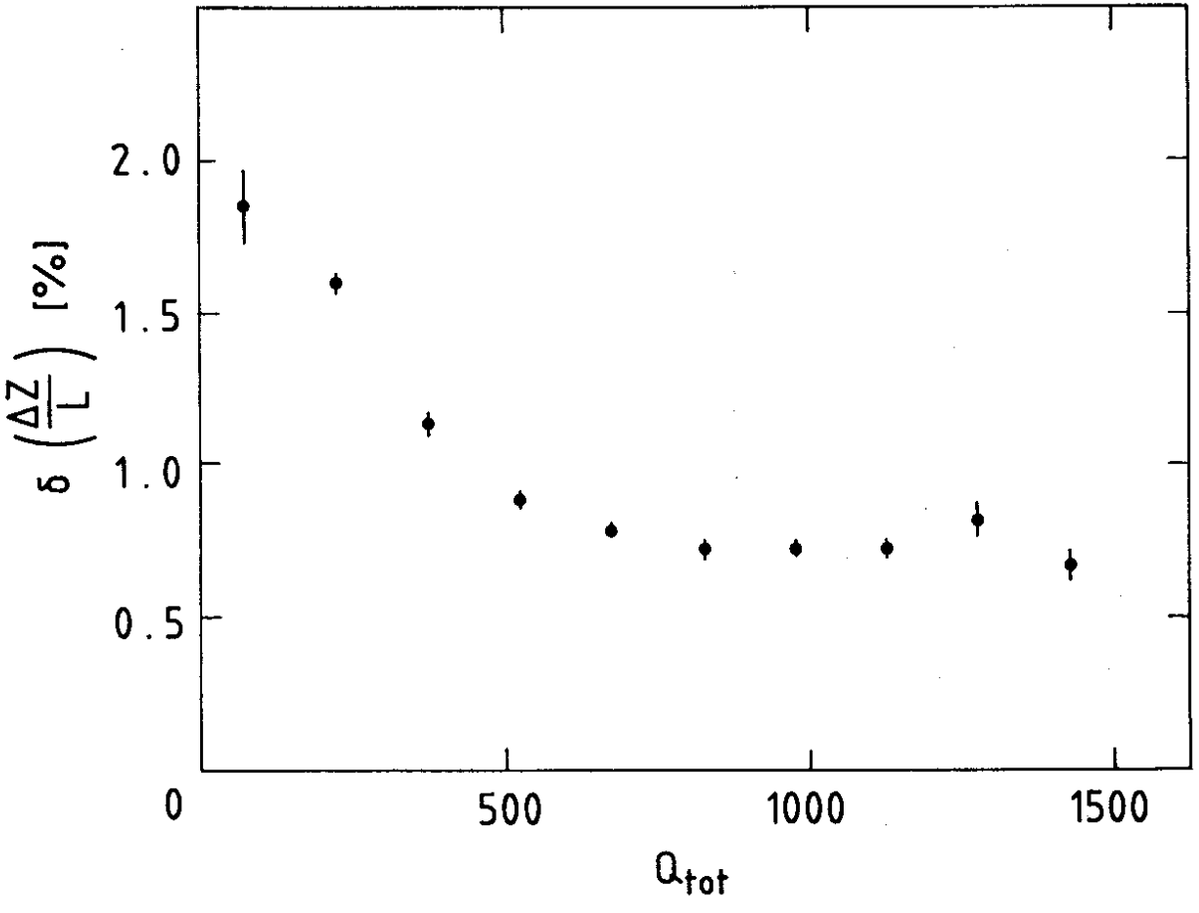


Fig. 6

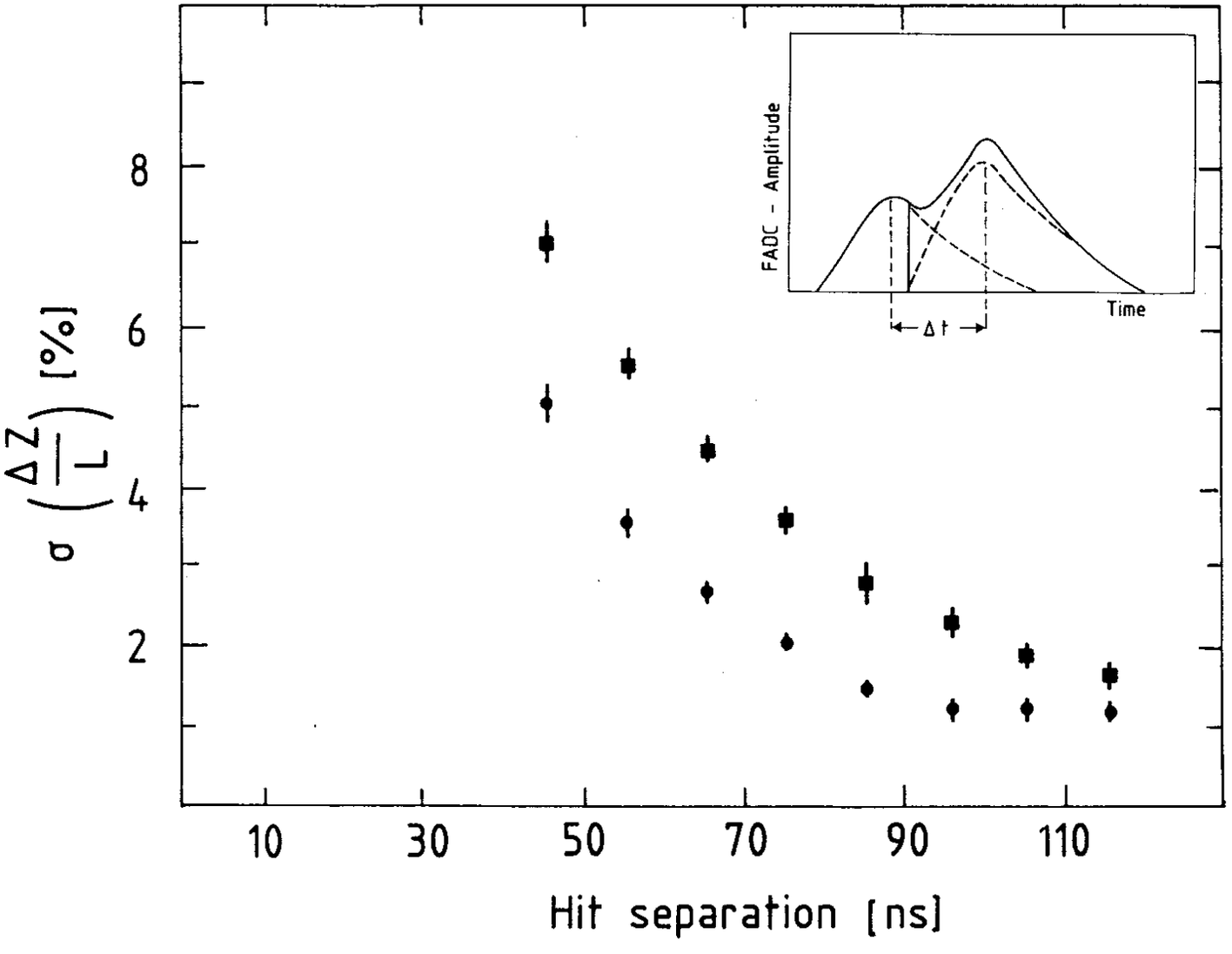
8
6
4
2
$\sigma\left(\frac{\Delta Z}{L}\right)$ [%]
10
30
50
70
90
110
Hit separation [ns]
FADC - Amplitude
Time
Δ t

Fig. 7

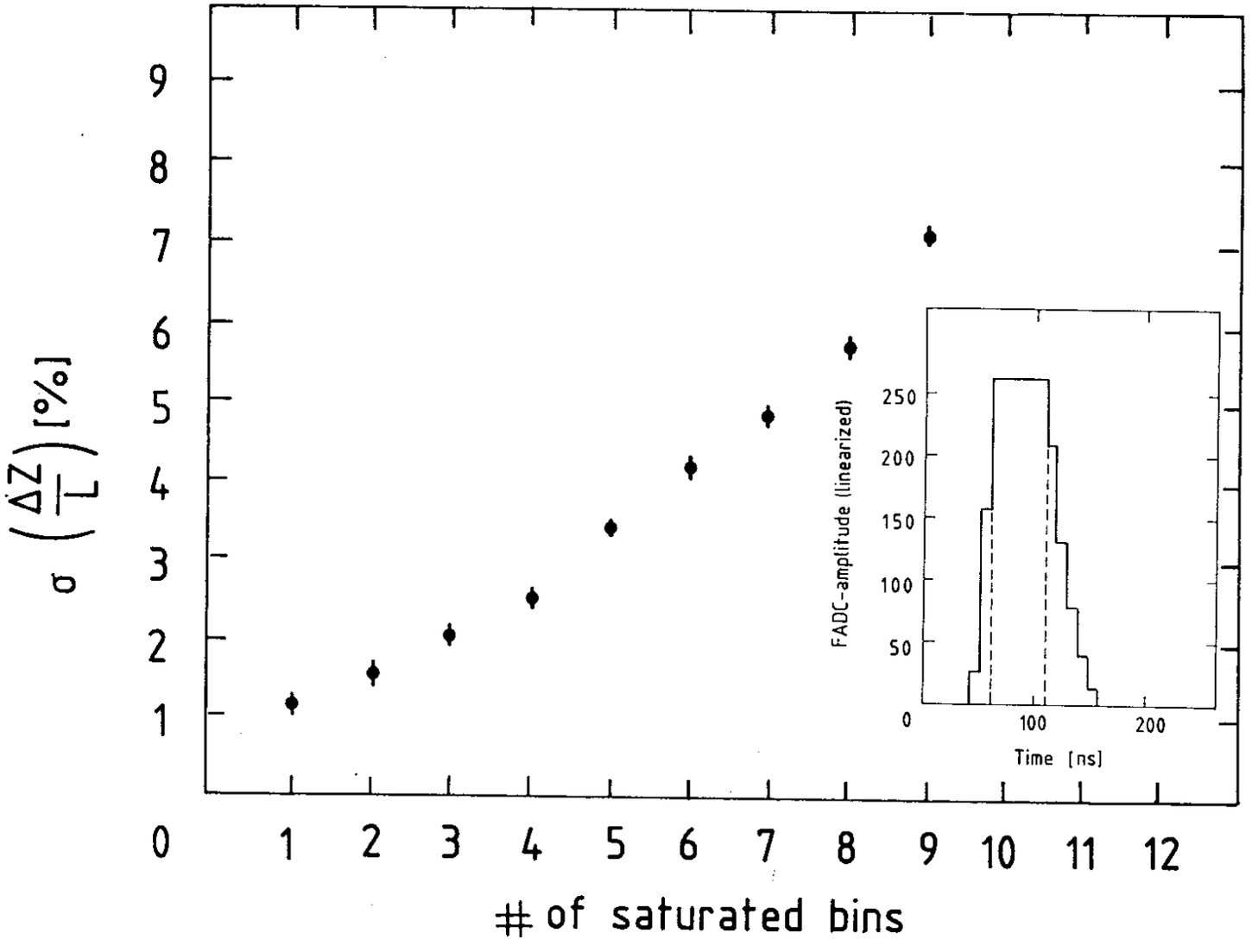
σ (ΔZ/L) [%]
9
8
7
6
5
4
3
2
1
0
1
2
3
4
5
6
7
8
9
10
11
12
# of saturated bins
FADC-amplitude (linearized)
250
200
150
100
50
0
100
200
Time [ns]

Fig. 8